63-4-1

BDM

15 APRIL 1963

DDC
JUL 10 1963
TISIA B

NANOSECOND PULSE BREAKDOWN STUDY

By
D. F. McDONALD and M. WALKER

Prepared For

ROME AIR DEVELOPMENT CENTER
RESEARCH AND TECHNOLOGY DIVISION
AIR FORCE SYSTEMS COMMAND
GRIFFISS AIR FORCE BASE
NEW YORK

BRADDOCK, DUNN & McDONALD, INC.   EL PASO, TEX

FOR ERRATA

AD _____

407469

THE FOLLOWING PAGES ARE CHANGES

TO BASIC DOCUMENT

BRADDOCK, DUNN AND MᶜDONALD, INC.

SUITE 1405 FIRST NATIONAL BUILDING · EL PASO, TEXAS
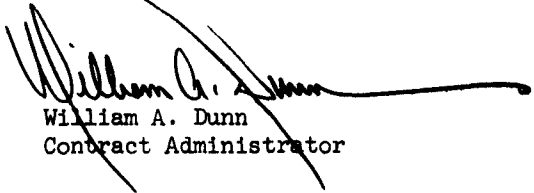
LIBERTY 2-1637

21 August 1963

TO: Distribution

SUBJECT: Replacement Pages for Report No.
RADC-TDR-63-201, Contract
AF30(602)-2781

    The enclosed replacement pages should be inserted in the
subject report as indicated, and the replaced pages should be
destroyed.

BRADDOCK, DUNN AND MCDONALD, INC.

William A. Dunn
Contract Administrator

WAD:mr

Enclosures:
    Cover, Title Page, and Page iii of Subject Report

Distribution:
    See Attached List

DISTRIBUTION LIST FOR CONTRACT REPORTS

<div align="right">Copy No.</div>

RADC (RALTP), ATTN: W. Quinn
Griffiss AFB NY   1-3

RADC (RAAPT)
Griffiss AFB NY   4

RADC (RAALD)
Griffiss AFB NY   5

GEEIA (ROZMCAT)
Griffiss AFB NY   6

RADC (RAIS, ATTN: Mr. Malloy)
Griffiss AFB NY   7

U. S. Army Electronics R&D Labs
RADC
Griffiss AFB NY   8

AUL (3T)
Maxwell AFB Ala   9

ASD (ASAPRD)
Wright-Patterson AFB Ohio   10

Chief, Naval Research Lab
ATTN: Code 2027
Wash 25 DC   11

Air Force Field Representative
Naval Research Lab
ATTN: Code 1010
Wash 25 DC   12

Commanding Officer
U. S. Army Electronics R&D Labs
ATTN: SELRA/SL-ADT
Ft. Monmouth NJ   13

National Aeronautics & Space Admin
Langley Research Center
Langley Station
Hampton Virginia
ATTN: Librarian   14

AMFTC (Tech Library MU-135)
Patrick AFB Fla   28

Central Intelligence Agency
ATTN: OCR Mail Room
2430 E Street NW
Wash 25 DC   29

US Strike Command
ATTN: STRJ5-OR
Mac Dill AFB Fla   30

AFSC (SCSE)
Andrews AFB
Wash 25 DC   31

Commanding General
US Army Electronic Proving Ground
ATTN: Technical Documents Library
Ft Huachuca Ariz   32

DDC (TISIA-2)
Arlington Hall Station
Arlington 12 Va   33 (10)

AFSC (SCFRE)
Andrews AFB
Wash 25 DC   34

Hq USAF (AFCOA)
Wash 25 DC   35

AFOSR (SRAS/Dr. G. R. Eber)
Holloman AFB NMex   36

Office of Chief of Naval Operations (Op-724)
Navy Dept
Wash 25 DC   37

Commander
US Naval Air Dev Cen (NADC Lib)
Johnsville Pa   38

Commander
Naval Missile Center
Tech Library (Code No. 3022)
Pt. Mugu Calif   39

AMFTC (Tech Library MU-135)
Patrick AFB Fla   28

Central Intelligence Agency
ATTN: OCR Mail Room
2430 E Street NW
Wash 25 DC   29

US Strike Command
ATTN: STRJ5-OR
Mac Dill AFB Fla   30

AFSC (SCSE)
Andrews AFB
Wash 25 DC   31

Commanding General
US Army Electronic Proving Ground
ATTN: Technical Documents Library
Ft Huachuca Ariz   32

DDC (TISIA-2)
Arlington Hall Station
Arlington 12 Va   33 (10)

AFSC (SCFRE)
Andrews AFB
Wash 25 DC   34

Hq USAF (AFCOA)
Wash 25 DC   35

AFOSR (SRAS/Dr. G. R. Eber)
Holloman AFB NMex   36

Office of Chief of Naval Operations (Op-724)
Navy Dept
Wash 25 DC   37

Commander
US Naval Air Dev Cen (NADC Lib)
Johnsville Pa   38

Commander
Naval Missile Center
Tech Library (Code No. 3022)
Pt. Mugu Calif   39

Bureau of Naval Weapons
Main Navy Bldg
Wash 25 DC
ATTN: Technical Librarian, DL1-3   40

RTD (RTH)
Bolling AFB
Wash 25 DC   41

Space Sciences, Inc.
ATTN: Dr. Joseph Proud
2 Mercer Road
Natick, Massachusetts   42

Microwave Associates, Inc.
ATTN: Dr. Meyer Gilden
Burlington, Massachusetts   43

NANOSECOND PULSE BREAKDOWN STUDY

By

D. F. McDONALD and M. WALTER

BRADDOCK, DUNN & McDONALD, INC.

EL PASO, TEXAS

Prepared For

ROME AIR DEVELOPMENT CENTER
RESEARCH AND TECHNOLOGY DIVISION
AIR FORCE SYSTEMS COMMAND
UNITED STATES AIR FORCE
GRIFFISS AIR FORCE BASE
NEW YORK

NANOSECOND PULSE BREAKDOWN STUDY

Daniel F. McDonald
Manfred Walter

BRADDOCK, DUNN AND McDONALD, INC.

Suite 1405
First National Building
El Paso, Texas

BRADDOCK, DUNN AND MCDONALD, INC.

ABSTRACT

The theory and most recent experimental work on breakdown under
high-power microwave pulses are analyzed. Recommendations are made
for further theoretical and experimental investigations to extend
this work into the nanosecond region. The feasibility of spectro-
scopic techniques in the study of discharge growth is considered.
It is shown that light emitted during discharge build-up may be of
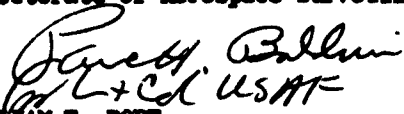sufficient intensity to allow photometric measurements of the growth
rate.

PUBLICATION REVIEW

This report has been reviewed and is approved.

Approved:

ARTHUR J. FROHLICH
Chief, Techniques Laboratory
Directorate of Aerospace Surveillance & Control

Approved:

WILLIAM T. POPE
Acting Director
Director of Aerospace
Surveillance & Control

FOR THE COMMANDER:

IRVING J. GABELMAN
Director of Advanced Studies

BDM

Braddock, Dunn and McDonald, Inc.

Suite 1405
First National Building
El Paso, Texas

15 April 1963

Nanosecond Pulse Breakdown Study

Daniel F. McDonald
Manfred Walter

BDM Report No. BQ 101
Contract No. AF 30(602) - 2781

Prepared for

Rome Air Development Center
Research and Technology Division
Air Force Systems Command
United States Air Force

Griffiss Air Force Base
New York

FOREWORD

Efforts to increase significantly the peak power levels of pulsed microwave systems have met a number of stubborn technical roadblocks. The demand for greatly increased peak power levels is so great, however, as to justify intense efforts to establish breakthrough techniques in all areas in which these have been encountered.

A well-known limitation of high-power systems is gaseous breakdown. Although much is known of this phenomenon for DC and microsecond pulse systems, breakdown mechanisms have not been studied extensively for the nanosecond pulse case. Since a number of technical considerations suggest improved performance for reduced pulse widths, more intensive theoretical and experimental efforts in the nanosecond region are clearly warranted. This report presents the results of a theoretical investigation of nanosecond microwave discharges and analyses of special diagnostic techniques for experimental studies.

ABSTRACT

The theory and most recent experimental work on breakdown under
high-power microwave pulses are analyzed. Recommendations are made
for further theoretical and experimental investigations to extend
this work into the nanosecond region. The feasibility of spectro-
scopic techniques in the study of discharge growth is considered.
It is shown that light emitted during discharge build-up may be of
sufficient intensity to allow photometric measurements of the growth
rate.

TABLE OF CONTENTS

Page

LIST OF ILLUSTRATIONS

INTRODUCTION

Voltage breakdown is a basic phenomenon which can limit the design of high-power microwave transmitting systems. Breakdown may occur in portions of the transmitter plumbing, at the transmitting antenna, or possibly in regions of free space where special conditions of local pressure and microwave power concentration obtain.

A number of experimental and theoretical studies have been conducted on microwave breakdown characteristics in waveguides and antennas.[1-6] Most of these have considered CW operation or pulses of about 1 μ sec. Many of these studies have considered only complete breakdown, where the impedance change in the breakdown region causes total reflection of the incident microwave power. Some have considered the growth characteristics of the discharge, but both theoretical and experimental information in this area is limited, especially where full breakdown occurs in nano-seconds. It may be possible, however, to take advantage of the finite growth at the discharge and transmit high-power nanosecond pulses before the discharge can go to completion.

To evaluate the possibility of transmitting high power levels during the formative time of the discharge, theoretical analyses of the discharge initiation and growth processes are required. In addition, experimental investigations using nanosecond pulses are also needed and these will require special experimental techniques. This report presents the results of theoretical investigations of the temporal growth of the discharge and studies of the feasibility of special diagnostic techniques for use in experimental work with nanosecond pulses.

I. THEORY OF DISCHARGE GROWTH

Theoretical and experimental work over the past 15 years has led to a basic understanding of the growth characteristics of microwave discharges. This applies particularly to the case of the low pressure, DC and microsecond pulse region. This section presents the mathematical model of breakdown which is generally accepted. The applicability of this theory to the high-pressure, nanosecond pulse region is then discussed.

A. Assumptions

Most theoretical approaches to the analysis of the growth of the microwave discharge are based on the assumption that the free electron density in the discharge is controlled by three processes:

1. Primary ionization of the gas by free electrons -- electron motion under field acceleration produces positive ions and free electrons, adding to the electron density.

2. Electron attachment to neutral molecules - this removes free electrons from the discharge region and forms negative ions.

3. Electron diffusion -- causes loss of free electrons from the discharge region by migration.

Based on these assumptions, a relatively simple model of the breakdown process can be developed. Note that ions are not considered as ionizing agents. This is due to the low mobilities of ions compared with electrons. Caution in neglecting ions as ionizing agents may be warranted in cases where extremely high electric fields are involved.

B. Discharge Growth Equation

Using the assumptions given in Section A, the following partial differential equation may be written, expressing the instantaneous rate of change of free electron density, n, as a function of position and time:

$$\frac{\partial n}{\partial t} = \nu_i n - \nu_a n + \nabla^2 Dn \qquad (1)$$

where

t - time in sec

n - free electrons/ cm^3

ν_i - ionization frequency

ν_a - attachment frequency

D - diffusion coefficient in cm^2/sec

For simple cases, this equation may be solved. One case in which the electric field configuration is similar to that of practical cases is that of a uniform field between plane parallel plates. It is shown in Figure la. The TE_{10} mode for rectangular guide is shown in Figure lb for comparison. For the field of Figure la, the electron density is a function of t and x only. Equation (1) may be solved by assuming a solution of the form

$$n(x,t) = T(t) \, X(x) \qquad (2)$$

where T is a function only of t and X is a function only of x.

Substituting Equation (2) in Equation (1) and separating variables leads to the following two ordinary differential equations:
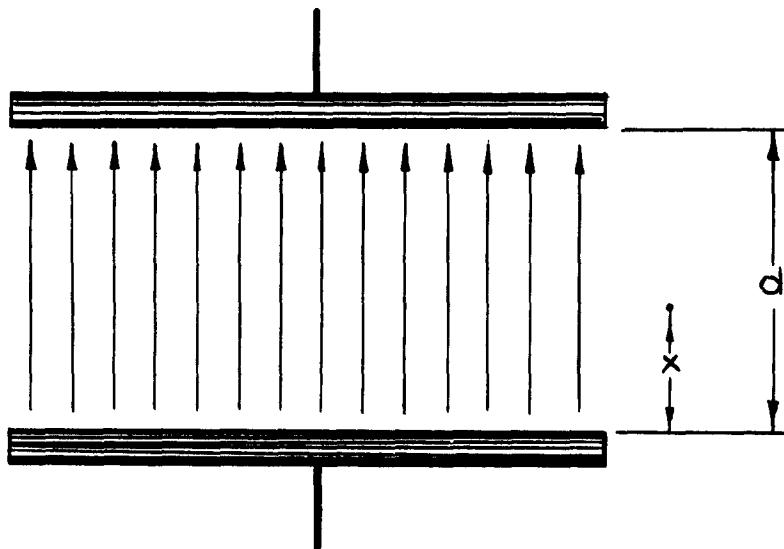
Figure 1a - Uniform field between parallel plates
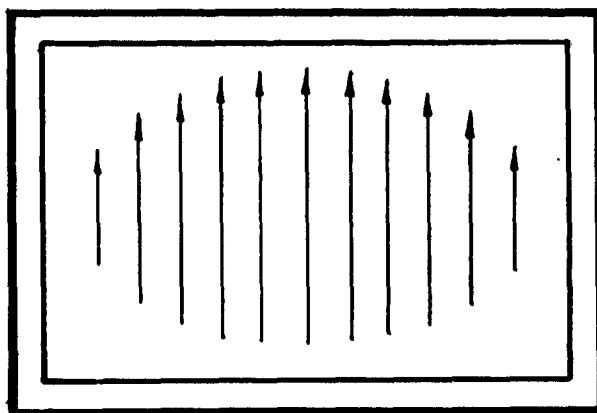
Figure 1b - TE_{10} Mode in rectangular guide

$$\frac{dT}{dt} = (\nu_i - \nu_a + C) \; T \tag{3}$$

$$\frac{d^2X}{dx^2} = \frac{C}{D} X \tag{4}$$

where C is the separation constant.

Particular solutions of these equations are:

$$T = T_k \epsilon^{\int_0^t (\nu_i - \nu_a - k^2 \frac{\pi^2}{d^2} D) dt} \tag{5}$$

$$X = B_k \sin \frac{k\pi}{d} x \tag{6}$$

In these solutions the boundary conditions (n = o at x = o and x = d) are met by making $C = \frac{k\pi^2}{d^2} D$ and k always an integer.

From the particular solutions a general solution may be formed as follows:

$$n(x,t) = \sum_{k=1}^{\infty} T_k B_k \epsilon^{\int_0^t (\nu_i - \nu_a - k^2 \frac{\pi^2}{d^2} D) dt} \times \sin \frac{k\pi x}{d} \tag{7}$$

This may be written as

$$n(x,t) = \epsilon^{\int_0^t (\nu_i - \nu_a) dt} \sum_{k=1}^{\infty} A_k \epsilon^{-\frac{k^2 \pi^2 D}{d^2}} \sin \frac{k\pi x}{d} \tag{8}$$

where $A_k = T_k B_k$

If the initial electron distribution, n, is uniform, it may be shown that

$$A_k = \frac{4n_0}{\pi k} \quad \text{for } k = 1, 3, \ldots$$

and

$$A_k = 0 \quad \text{for } k = 2, 4, \ldots$$

Thus n may finally be written as

$$n(x,t) = \frac{4n_0}{\pi} \in^{\int_0^t (\nu_i - \nu_a)dt} \sum_{k=1}^{\infty} A_k \in^{-\frac{k^2\pi^2 D t}{d^2}} \sin \frac{k\pi x}{d} \tag{9}$$

Inspection of Equation (9) shows that the higher modes in the density distribution reduce sharply in importance as time progresses. In the analysis presented in Reference 4, only the fundamental mode is considered, giving n as

$$n = \frac{4n_0}{\pi} \in^{\int_0^t (\nu_i - \nu_a)dt - \frac{\pi^2 D t}{d^2}} \times \sin \frac{\pi x}{d} \tag{10}$$

Thus the density distribution at any point, x, grows with time for the case of

$$\int_0^t (\nu_1 - \nu_a)dt - \frac{\pi^2 D t}{d^2} > 0 \tag{11}$$

In considering breakdown under pulse, the Equation (10) is extremely useful, since it allows the determination of the time taken to reach the critical electron density, n_b, at which significant microwave energy is reflected from the discharge volume. This electron density is reached at a time t_b where

$$n_b = \frac{4n_0 \epsilon}{\pi} \int_o^{t_b} (\nu_i - \nu_a) dt - \pi^2 \frac{D}{d^2} t_b \tag{12}$$

If this time involves several cycles of rf, then we may write

$$\int_o^{t_b} (\nu_i - \nu_a) dt \cong \langle \nu_{net} \rangle t_b \tag{13}$$

where $\langle \nu_{net} \rangle$ is the average value of $\nu_i - \nu_a$ over a full cycle of rf and represents the average net ionization.

To analyze quantitatively the growth characteristics for a particular gas and a particular microwave power level, the value of $\langle \nu_{net} \rangle$ must be determined. This may be done by determining the variation of electron energy over a full cycle for the given conditions of pressure and peak field strength. When this is known, the variation of $\langle \nu_{net} \rangle$ over a complete cycle of rf may be determined from available DC measurements of these quantities. Finally, the values of the diffusion coefficient, D, can be determined from the well-known relationship

$$D = \frac{2}{3} u\mu$$

where u and μ are the electron energy and mobility respectively.

C.   Theoretical Predictions for Breakdown in Air

In work supported by the Bureau of Ships under Contract NObsr-63295, Gould and Roberts at Microwave Associates, Inc. have carried out the calculations of ν_{net} for a number of values of E/p, where E is the electric field strength in volts/cm and p is the pressure in mm Hg. They assumed that breakdown occurs when $n_b/n_\bullet$ is equal to 10^8. With this information and the diffusion constant, D, they were able to establish theoretical breakdown curves for various pulse widths, pressures, and electrode spacing using Equation (10).

The work of Gould and Roberts is summarized in the HANDBOOK ON BREAKDOWN OF AIR IN WAVEGUIDE SYSTEMS published by Microwave Associates, Inc. in April, 1956. A graph taken from that document is reproduced in this report under Figure 2. The information on this graph is used directly to calculate the breakdown field intensity for pulses of various widths and the TE_{10} mode in rectangular guide. The field configuration for this mode is similar to that assumed in the theoretical breakdown model.

Using the information presented in Figure 2, it is possible to compare the breakdown power levels predicted by theory for microsecond versus nanosecond pulse widths. This has been done for the case of a rectangular guide type RG-48, microwave frequency of 2.8 kmc, and air at atmospheric pressure. The results are as follows:

Case 1 - Pulse Width - 1.0 microseconds
           Breakdown at 12.2 megawatts

Case 2 - Pulse Width - 3 nanoseconds
           Breakdown at 93.5 megawatts
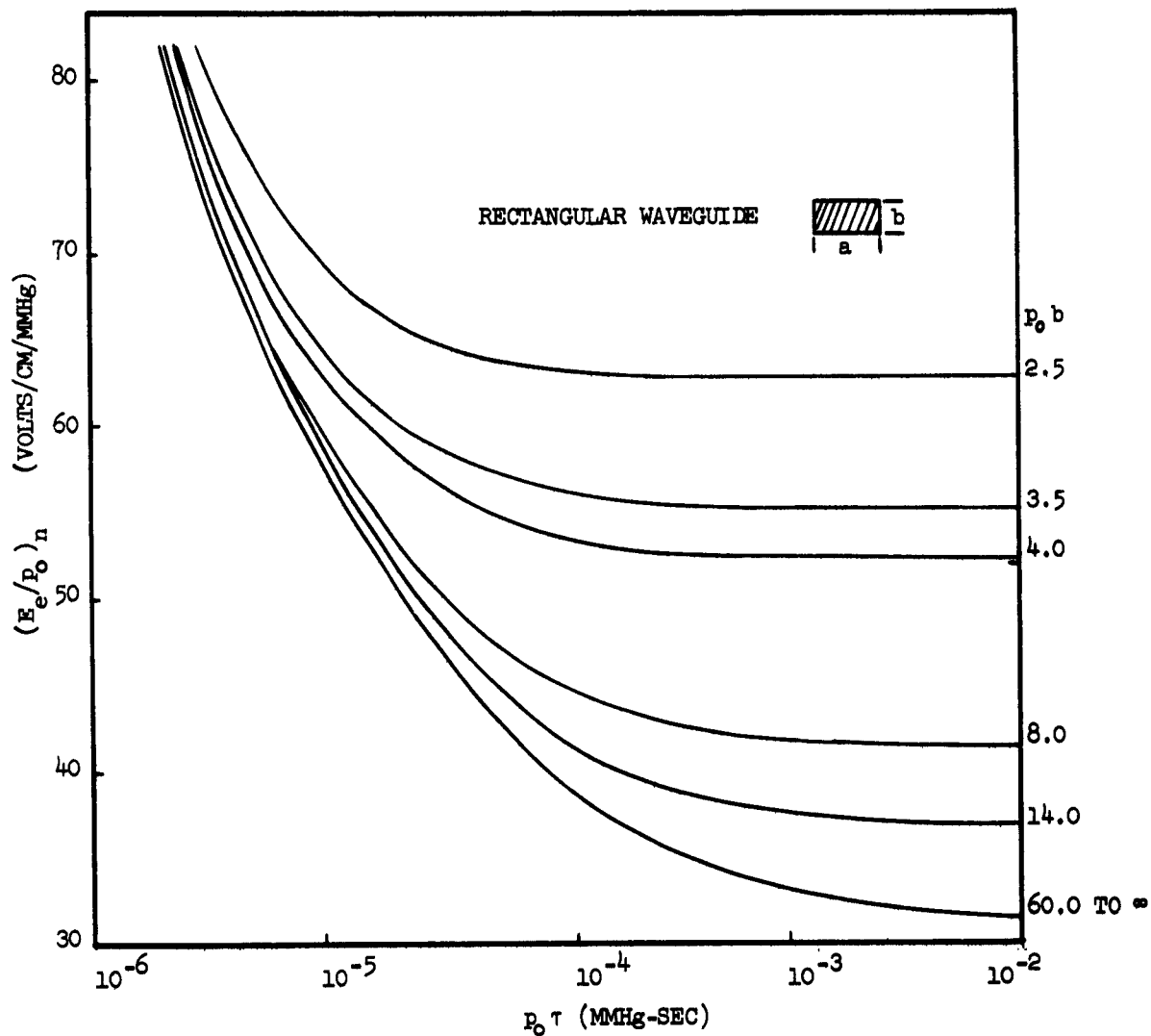
Figure 2 - Theoretical normalized single pulse breakdown curves.

The comparison of the results of these two cases shows that theory does indeed predict a considerable improvement in the peak power capabilities for nanosecond versus microsecond pulses. These power levels are unusually high compared with those typically listed with standards for waveguides. Listed ratings are based on CW operation and the breakdown rating of 10 kv/cm rms field strength. For RG-48 guide, these criteria lead to CW power ratings of about 3 megawatts.

From the theoretical model and its predictions, it is clear that considerably greater peak power may be transmitted as pulse widths are reduced toward the nanosecond region. This result is very promising and suggests further refinements in the mathematical model of breakdown, as well as more intensive experimental verifications of its predictions. Some of the experimental work which has been done is discussed in the following sections.

D.   Experimental Studies of Pulse Breakdown

Gould and Roberts[4] have reported the results of experimental microwave pulse breakdown studies. These studies used pulse widths of 0.8, 2.5 and 4.0 microseconds at a frequency of 2.8 KMc. The test cell in which breakdown was measured was a cylindrical microwave cavity whose height was 0.635 centimeters. Pressures were varied from 21 to 1600 millimeters Hg.

The experimental results of Gould and Roberts agrees well with their theoretical curve. The use of a high-Q resonant cavity and short pulses does warrant some comment. The cavity used had a Q of 1,000.* This implies a cavity filling time of 0.06 μ sec for the frequency used. The energy in the cavity as a function of the time of application of the pulse is given approximately by

*L. W. Roberts, Private Communication, 1 April 1963

$$P_i \tau \left(1 - \epsilon^{-\frac{t}{\tau}}\right) \tag{14}$$

where $\tau = \dfrac{Q}{2\pi f}$ and P_i is the input or waveguide power level.

The electric field intensity, which is of more direct interest, is related to energy density as follows

$$E \sim (P_i \tau)^{1/2} \left(1 - \epsilon^{-\frac{t}{\tau}}\right)^{1/2} \tag{15}$$

For the case of $Q = 1,000$ and $f = 2.8$ kmc the value of τ is 0.06 μsec. For the shortest pulse width (0.8 μsec) used by Gould and Roberts, cavity rise time is short compared to the pulse rise time. The rise time of the energy density in the cavity is then determined by the pulse rise time alone. If work is to be done with nanosecond pulses, considerably shorter values of τ must be employed. It may develop that the cavity resonator technique is not suitable from this point of view.

Where cavity resonator techniques are used, the electric field intensity within the cavity is determined indirectly from measurements of other parameters in the experimental system.[7,8] Gould and Roberts do not make explicit reference to this in their publication but it is presumed these techniques were used. It should be noted that since energy stored in the cavity depends on $P_i \dfrac{Q}{2\pi f}$ that accurate measurements of Q are indeed very important.

Another point which should be mentioned is the guide-cavity coupling. This involves stubs and apertures. Since these represent a departure from the ideal geometry of the cavity, breakdown may occur at the edges of apertures or stubs. This effect could yield lower breakdown values than the ideal case.

The work of Gould and Roberts says much about pulse breakdown and deserves close critical attention. It is a point of departure for nanosecond breakdown studies, but much further experimental work is needed. This work should emphasize:

1. Pulse widths of 1 to 100 ns
2. Improved test cell techniques
3. Increased effort to record breakdown growth

E. High Field Values of ν_{net}

In the preceding discussions, it was emphasized that the values of ν_{net} determined the breakdown growth rate. To calculate values of ν_{net} the instantaneous values of the electron energy u are required. The differential equation determining u is

$$\frac{du}{dt} = \frac{\mu E_o^2}{1 + (\omega/\nu_c)^2} \left[\sin^2 \omega t - \frac{\omega}{2\nu_c} \sin \omega t \right] - K\rho\mu$$

where E is the peak field value, ν_c is the collision frequency and K is the fractional energy loss/sec - mm Hg. For a particular gas this equation is integrated numerically, relating u to the phase of the microwave field. Then from DC measurements, both ν_i and ν_a are related to u and hence to the phase of the microwave field. The values of $\nu_i - \nu_a$ are then averaged over one cycle to yield a value of $<\nu_{net}>$.

For the microwave power levels under consideration, the peak values of the electric field may be 60,000 volts/cm or even greater. None of the DC experiments used to measure ionization and attachment coefficients use such high fields. Usually, field intensities of a few hundred volts/cm are employed. The DC data, however, are presented as functions of

the ratio E/p. It is assumed that the data apply to this ratio, regardless of the absolute value of E. Thus, for example, a measurement made at 250 volts/cm and 5 mm Hg is assumed to apply to the case of 50,000 volts/cm and 1,000 mm Hg. This extrapolation certainly warrants considerable scrutiny.

F.   Breakdown in Sulphur Hexafluoride

Air and sulphur hexafluoride are the most widely used dielectric gases. The characteristics of sulphur hexafluoride suggest that it would have an unusually low value of $<\nu_{net}>$ and that much higher breakdown power levels with sulphur hexafluoride would be realized than are realized with air. Considerable work has been done comparing breakdown in air with breakdown in SF_6. It would be useful to apply the breakdown theory presented in the preceding sections to SF_6.

Some of the material on SF_6 attachment and ionization coefficients and other characteristics which was developed during this study is presented in the Appendix.

II.   NATURAL ELECTRON DENSITY AND BREAKDOWN INITIATION

In all theories of microwave and DC gas discharges, it is assumed
that there is an initial electron or an electron concentration in the
gas volume under study. The initial free electron or free electrons
become the agents which first produce increasing ionization in the gas
under the action of the electric field. These initial free electrons
are produced by external agencies such as radioactive material and
cosmic radiation. The relationship of electron density and discharge
initiation is discussed in this section.

A.   Natural and Artificial Conditions

For the case where experimental studies of breakdown are
conducted without the use of auxiliary radiation sources such as
Cobalt 60, considerable statistical lags are observed in the initiation
of microwave discharges. In most pulse studies, this statistical effect
manifests itself as an intermittent breakdown effect. Breakdown occurs
only for a fraction of the total number of pulses transmitted. For
those pulses in which breakdown does not occur, it is assumed that free
electron concentration in the volume under study was not at sufficient
levels during the pulse period to lead to breakdown.

In other laboratory experiments on microwave discharges, high
initial electron concentrations are artificially induced using Cobalt
60 or other sources of radioactivity. These radioactive sources may
raise initial electron concentration levels as high as 10^3 electrons
per cc. In the experimental work of Gould and Roberts, this technique
eliminated statistical fluctuation in breakdown initiation and permitted

correlation of observed breakdown and the theory which assumes high initial electron concentrations. This, therefore, was a laboratory experiment which may not have been realistically related to the field case.

The mechanism of discharge initiation and the statistics associated with it may be basic to the investigation of techniques for transmitting super-power nanosecond microwave pulses. For example, in going from the microsecond pulse widths to the nanoseconds pulse widths, the probability of transmitting pulses without breakdown improves by a factor of 100 to 1000.

B.   Analysis of Free Electron Concentration

In the absence of an artificial ionizing radiation source, free electron concentrations in a gas sample are extremely low. It is generally assumed that those which do exist are due to the high energy radiation in cosmic rays and natural radioactivity in the walls of the test chamber. In most cases, the ionizing agents in the gas sample are secondary electrons ejected from the walls into the chamber by the high energy radiation. These electrons ionize the molecules of the gas. In the case of air, this results in the formation of ions at the rate of about 10 ion pairs/cm^3 - sec. Free electrons generally appear in groups numbering from 1 to 10 electrons. Thus, there are one or two ionizing events /cm^3 - sec in a specimen volume, each event contributing about 5 electrons.

When ionization occurs, an electron is ejected from one of the constituent molecules of the gas, forming a positive ion and a free electron. In most cases, the free electron quickly attaches itself to a neutral molecule forming a negative ion. This will normally occur in times of 10^{-7} seconds or much less. The resulting ions have much longer lives lasting for times of the order of ten's to hundred's of seconds.

It is interesting to estimate the expected lifetime of free electrons due to high-energy radiation in a typical waveguide structure such as RG-48. Estimates of this lifetime may be arrived at as follows:

For free electrons whose energies are between 0 and 2.0 electron volts, the average attachment coefficient is about 2×10^{-5}/collision. At one electron volt, the electron speed is 6×10^7 cm/sec. At atmospheric pressure, it experiences about 3×10^4 collisions per centimeter. Thus, on the average, a free electron will travel 1.7 cm before attaching. It travels the distance in the time of 3×10^{-8} sec.

For free electrons with energies between 2.0 and 50,000 volts, in air the average ranges are a few centimeters and average speeds of about 5×10^8 cm/sec. Thus, the time for the electron energy to fall to 2.0 volts or less is about 10^{-8} seconds.

For free electrons with energies above 50,000 volts, the ranges vary from a few cms to meters. Speeds are near the speed of light. Thus, these electrons pass through the discharge chamber into a wall in a few nanoseconds.

From these order of magnitude calculations, it appears that free electron lifetimes are of the order of 10^{-8} sec in a typical waveguide at atmospheric pressure.*

Taking 10^{-8} sec as the lifetime of a free electron at atmospheric pressure and assuming that there are only 2 ionizing events/sec/cm^3, it is clear that there is a low probability that free electrons will be present during a short pulse. For a microwave pulse, of width τ which is large compared to 10^{-8} sec, it may be shown that the probability of free electrons being available to initiate discharge during the pulse period is approximately

$$P = 2V\tau$$

where V is the volume of the discharge chamber and there are two ionizing events/cm^3.

Taking this as a probability of breakdown, we can calculate P for typical cases. In the work of Gould and Roberts, the volume of the test cell was about 6 cm^3. Pulse widths were 0.8, 2.5, and 4.0 μ sec. This leads to probability of breakdown of the order of

2×10^{-5} breakdown/pulse

Gould and Roberts observed, however, that the breakdown probability was 10^{-3}.

*This is order of magnitude only and it is noted that published estimates, e.g., by Compton and Langmuir, Rev. Mod. Phys. 2,193 (1930) are between 10^{-6} and 10^{-7} sec.

It is very important to investigate this difference between the expected and observed probability of breakdown. This investigation should include the following:

1. Examination of the role of ions in initiating discharge
2. Role of surface effects
3. Role of contaminants such as dust

In general, a much deeper understanding of how breakdown occurs may lead to techniques to inhibit the initiating process. Such techniques may be concerned with surface conditions, contaminants, reducing radioactive content of materials, or other factors. They could be used to improve greatly the statistical probability of transmitting super-power pulses of nanosecond widths.

III. DIAGNOSTIC TECHNIQUES IN DISCHARGE INVESTIGATIONS

A. Introduction

The experimental techniques used typically in studying the growth of microwave discharges have provided limited information about the temporal growth of the discharge. Measurements of reflected microwave energy have yielded information on the average free electron density in the discharge region. Improved nanosecond pulse techniques should lead to more detailed information in this area.

In this section, the feasibility of spectroscopic techniques is considered. Used successfully, these could contribute considerably more information about the increasing concentration of ion populations and the spatial distribution of the discharge in the test volume.

Both absorption and emission spectroscopy are considered.

B. Absorption Spectroscopic Techniques

For microwaves of wavelength λ, the discharge region becomes highly reflecting when the electron density reaches or exceeds the critical level, n_b, given as

$$n_b = \frac{10^{13}}{\lambda^2} \text{ electrons/cm}^3$$

where λ is in cms. Thus, at 3kmc, the critical level is

$$n_b = 10^{11} \text{ electrons/cm}^3$$

In the high-power nanosecond pulse case of interest here, the discharge will reach this level in 10^{-8} sec. In Section II, it was shown that free electron average lifetimes are of this order. Ion lifetimes are much longer. It then follows that when breakdown electron concentration is reached, the discharge region contains

10^{11} electrons/cm^3

10^{11} positive ions/cm^3

The positive ions are both O_2^+ and N_2^+ with the latter predominating.

To estimate the effectiveness of spectroscopic absorption techniques in measuring ion concentrations, the absorption cross-sections for O_2^+ and N_2^+ are needed. These are not readily available but, by assuming unusually favorable absorption characteristics, it is possible to show that a practical absorption technique is not possible.

Assume that the ions in the discharge have large cross-sections, around 10^{-19} cm^2, and absorption spectra located in the visible. Then the absorption of a test beam of intensity I is given by

$$\frac{dI}{I} = -\sigma\rho dx$$

where σ is the absorption cross-section and ρ is the ion density. For the values of σ and ρ which apply here this yields

$$dI = -10^{-8}\, dx$$

Thus, for a path length of 10 cms, as long as is practical, this yields

$$\frac{dI}{I} = -10^{-7}$$

The measuring photometer (probably a photomultiplier) must have a response time of about 1 ns to suitably resolve the experimental pulse rise. Thus in calculating signal-to-noise ratios, the signal sampling time is taken as 1 ns. If N is the total number of photons which pass through the test region in that time, then the signal S is the amount absorbed or

$$\text{Signal} = N \times 10^{-7}$$

The photon shot noise is given as

$$\text{Noise} = \sqrt{N}$$

Therefore

$$\text{Signal/Noise} = 10^{-7} \sqrt{N}$$

Let us assume this value to be 5 or greater; that is, the signal is fairly readable above the noise. Then we have that

$$N = 2.5 \times 10^{15} \text{ photons}$$

Since this number must pass through absorption region in 1 ns, this requires a beam intensity I of

$$I = \frac{N}{1 \text{ ns}} = 2.5 \times 10^{24} \text{ photons/sec}$$

Assuming a photon energy of 2.5×10^{-19} joules, this corresponds to an input peak light power of

$$P_1 = 100 \text{ kw}$$

Note that this does not allow for light collection or photon detection efficiency. When this is taken into account, the peak light power

requirement is 10 Mw or greater. This is an extremely high light
power level and would require a laser source. Since these calcu-
lations are based on the most favorable considerations, it appears
that the absorption spectroscopic techniques required for diagnostic
studies are well beyond the state of the art.

C.   Emission Spectroscopy

It is well known, of course, that there is strong emission
of light from a microwave breakdown. Most of this emission, however,
is associated with complete breakdown. There is considerably less
during breakdown growth. Analysis is presented in this section of
the feasibility of using the emission during growth to record the
growth rate.

In Section I, the expression, Equation 10, developed for the
free electron density at the center of the gap during discharge
growth may be written

$$n = \frac{4n_o}{\pi} e^{<\nu_{net}>t}$$

where high pressures (760 mm Hg) are assumed and diffusion losses
are negligible.

In the cases of interest breakdown occurs at $t \sim 10^{-8}$ sec.
Let us assume that the specimen gas is artificially ionized by
Co^{60} as in the case of Gould and Roberts' work. This gives values
of n_o of 10^2 to 10^3. Results of this analysis are not too sensitive
to this parameter and 10^2 is arbitrarily selected as the value of
$4n_o/\pi$. Thus we have at breakdown

$$10^{11} = 10^2 e^{+ \nu_{net} \times 10^{-8}}$$

This yields a value of ν_{net} of

$$\nu_{net} = 10^8 \ln 10^9$$

$$\nu_{net} = 2 \times 10^9 \text{ ionization/sec-electron}$$

Thus, we have the free electron density expressed as

$$n = 10^2 e^{2 \times 10^9 t}$$

If the air fluorescence decay time is longer than a few nano-
seconds, it will severly limit the resolution required in measuring
growth rate. However, it has been measured as 2.0 ns at atmospheric
pressure by several experimenters. Thus, it may be used directly to
measure growth rate without serious error. Since the decay of air
fluorescence is exponential, analytic techniques can be used to "sub-
tract out" the effects of fluorescence lifetime in the recorded signal
and yield more accurate growth measurements.

Next it is necessary to estimate the light power output from the
discharge region. This may be done by determining the power absorbed
by the region from the microwave field. At atmospheric pressure and
peak field intensities of 40,000 v/cm, the average velocity of free
electrons, v_d, is

$$v_d = 10^6 \text{ cm/sec}$$

$$10^{11} = 10^2 e^{+\nu_{net} \times 10^{-8}}$$

This yields a value of ν_{net} of

$$\nu_{net} = 10^8 \ln 10^9$$

$$\nu_{net} = 2 \times 10^9 \text{ ionization/sec-electron}$$

Thus, we have the free electron density expressed as

$$n = 10^2 e^{\, 2 \times 10^9 t}$$

If the air fluorescence decay time is longer than a few nano-seconds, it will severely limit the resolution required in measuring growth rate. However, it has been measured as 2.0 ns at atmospheric pressure by several experimenters. Thus, it may be used directly to measure growth rate without serious error. Since the decay of air fluorescence is exponential, analytic techniques can be used to "subtract out" the effects of fluorescence lifetime in the recorded signal and yield more accurate growth measurements.

Next it is necessary to estimate the light power output from the discharge region. This may be done by determining the power absorbed by the region from the microwave field. At atmospheric pressure and peak field intensities of 40,000 v/cm, the average velocity of free electrons, v_d, is

$$v_d = 10^6 \text{ cm/sec}$$

This gives a current density, j, of

$$j = env_d$$

where e is the electronic charge. The power absorbed per cm^3, P_v, is then given by

$$P_v = jE$$

$$= ev_d En$$

$$= ev_d En_0 e^{\nu_{net} t}$$

For the parameters used here this becomes

$$P_v = 4.7 \times 10^{-6} \text{ watts/cm}^3 \qquad \text{(1 ns)}$$

$$P_v = 3.1 \times 10^2 \text{ watts/cms}^3 \qquad \text{(10 ns)}$$

To determine the light output per cm^3, it is necessary to determine the conversion efficiency from electrical input power to light output power. McDonald and Dunn* estimated this as 10^{-5} on the basis of work done with 20kv electrons and air at atmospheric pressure. Although it is not certain that this applies to low voltage electrons as well, it will be used here for the purpose of estimation. Thus, light output power/cm^3 is

$$P_L = 4.7 \times 10^{-11} \text{ to } 3.1 \times 10^{-3} \text{ watts/cm}^3 \qquad \text{(1 ns to 10 ns)}$$

This corresponds to about

$$0.1 \text{ to } 10^7 \text{ photons per nanosecond/cm}^3 \qquad \text{(1 ns to 10 ns)}$$

*Unpublished

For sample volumes of 10 cm^3 and good collection efficiency, photomultiplier recording should begin to measure light output in 2 or 3 ns from the initiation of the discharge. As the discharge approaches complete breakdown, light signal levels will be easily recorded.

IV.   CONCLUSIONS

Conclusions

In the preceding sections, analyses were presented of the micro-wave pulse breakdown theory, experiments, and diagnostic techniques applicable to nanosecond breakdown studies. The following conclusions are drawn from the results of these analyses.

1. Current theory and experiment provides a satisfactory under-standing of the discharge growth in the high-power microsecond pulse region.

2. The results of current theory and experiment may be extrapolated to the nanosecond high-power pulse region, but experimental work using high-power nanosecond pulses directly is needed to verify theory for ultra-short pulses.

3. Test cell techniques may be a source of error in experimental work with pulse breakdown. Special experimental effort is required in this area.

4. Theoretical and experimental study of the ionization and attachment coefficients under high-field, high-pressure conditions is needed to provide a check on currently used values. Current values are determined under low-field, low-pressure conditions.

5. More theoretical analysis is required to establish the lifetimes and natural concentrations of free electrons in air and other gases. The mechanism of discharge initiation requires detailed investigations in this area and perhaps others.

6. Emission spectroscopic techniques may be feasible for studies of the discharge growth rate.

APPENDIX

Note on Sulphur Hexafluoride

The theory of microwave breakdown presented in Section I applies
to all gases. As was shown in the development of that theory, the
value of the average net ionization coefficient $<\nu_{net}>$ determined
the rate at which breakdown proceeds. This theory was applied to
the case of air which is of special interest because it is used
commonly in filling waveguides. The other gas which is also often
used is sulphur hexafluoride (SF_6).

Sulphur hexafluoride has unusual properties which make it a
particularly effective dielectric gas. In particular, it is
electronegative; i.e., it has a high attachment cross-section.
Thus, the value of ν_a can be very high and at the same time, the
ionization coefficient, ν_i, is very low. Thus, ν_{net} is generally
very small. Discharge growth is prevented or proceeds at a rate
much slower than for air under the same power levels. Aspects of
SF_6 considered during the breakdown study are presented here.

Electron Attachment in SF_6

This section covers the present knowledge of processes occuring upon collision between electrons and SF_6 - atoms and ions.

Figure 3 shows the octahedral symmetry of the SF_6 molecule, and its approximate dimensions. The normal valence of sulfur, 4, has been extended to 6, possibly indicating some fractional bond energy remaining between the fluorine atoms. Both bonds, the S-F and the possibly remaining F-F portion, are covalent; i.e., they are due to electron pair exchange forces. The bond energy of the S-F bond is estimated to 100 K cal mol^{-1} following data presented by Pauling [10]. This yields a total bond energy of approximately 500 K cal mol^{-1}, assuming some reduction of the SF bond energy due to the valence increase from 4 to 6. By comparison, the bond energies of other compounds featuring high strength bonds are:

$$H - F = 147 \text{ K cal mol}^{-1}$$

$$F - F = F_2^* \; 63.5 \text{ K cal mol}^{-1}$$

$$H - O = 220.3 \text{ K cal mol}^{-1}$$

$$H - F = H_2, \; 103.4 \text{ K cal mol}^{-1}$$

The above data show that the bond energy of the SF_6 molecule is very high and the molecular structure is a highly symmetrical dense package, exposing only strongly electronegative fluorine atoms on its surface. These properties are largely responsible for the high stability, chemical inertness (all bond-providing electron pairs are fully occupied within the molecule), and electron-attaching properties. The simplicity and symmetry of the bond structure, in conjunction with the
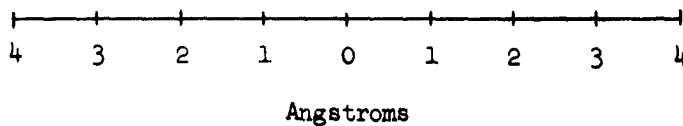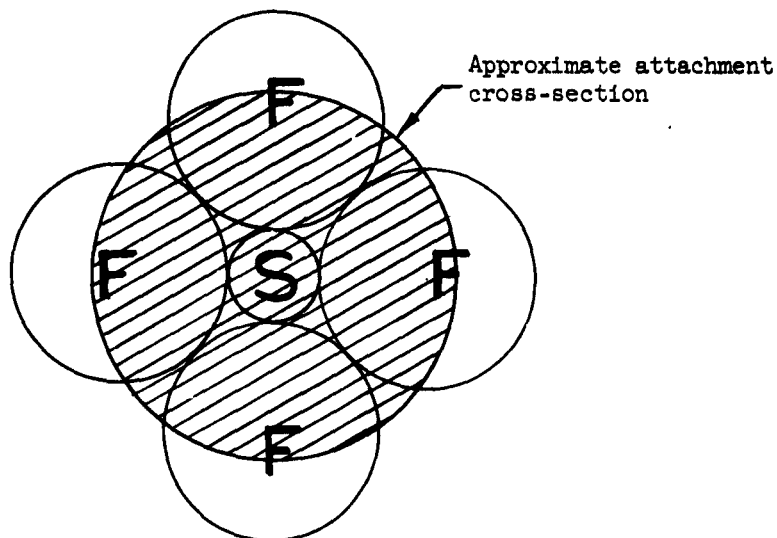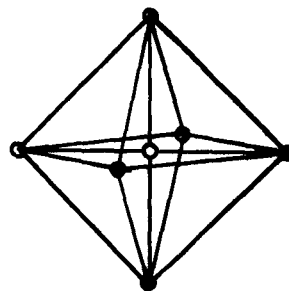
Octahedral arrangement
of fluorine atoms

Approximate attachment
cross-section

4   3   2   1   0   1   2   3   4

Angstroms

Fig 3.   Approximate Dimensions of SF_6 Molecule.

high bond strength, are probably responsible for the very small permanent and the low value of the induced dipole moment of SF_6.

The above information provides some understanding of the chemical and physical properties of SF_6 but indicate little towards its gaseous electronics properties. A few basic properties described above are borne out qualitatively, like the strong electron-attaching properties which can be expected from the dense highly symmetrical package of electronegative fluorine atoms surrounding the central sulfur atom. The chemical inertness suggests low decay rates in the hot environment of spark or arc discharges. Both properties are exhibited in a rather striking manner. The attachment cross-section of SF_6 for slow electrons is one of the highest known, 6×10^{-16} cm^2, which is approximately equal to the total cross-sectional area of the molecule (Figure 4). Decay rates in spark discharges through SF_6 have been found to be extremely small by one of its manufacturers. Only 5% of the gas was decomposed after 5 h of continous arcing in a waveguide.

The large attachment cross-section means that most slow electrons colliding with an SF_6 molecule stick to it, forming an SF_6^- ion. Thus, for electrons of thermal energy, the attachment coefficient is likely to be as high as 50%. With increasing electron energies, the attachment coefficient decreases rapidly, as indicated by the ion current measured in pertinent experiments.

According to Fox, [11] no ionization occurs between 2 and 12 ev; at approximately 12 ev, positive ions are first observed. In the region between these two energies there may be some energy transfer between the electrons and the rotational and/or vibrational states of the molecules or ions but not of a magnitude leading to ionization.
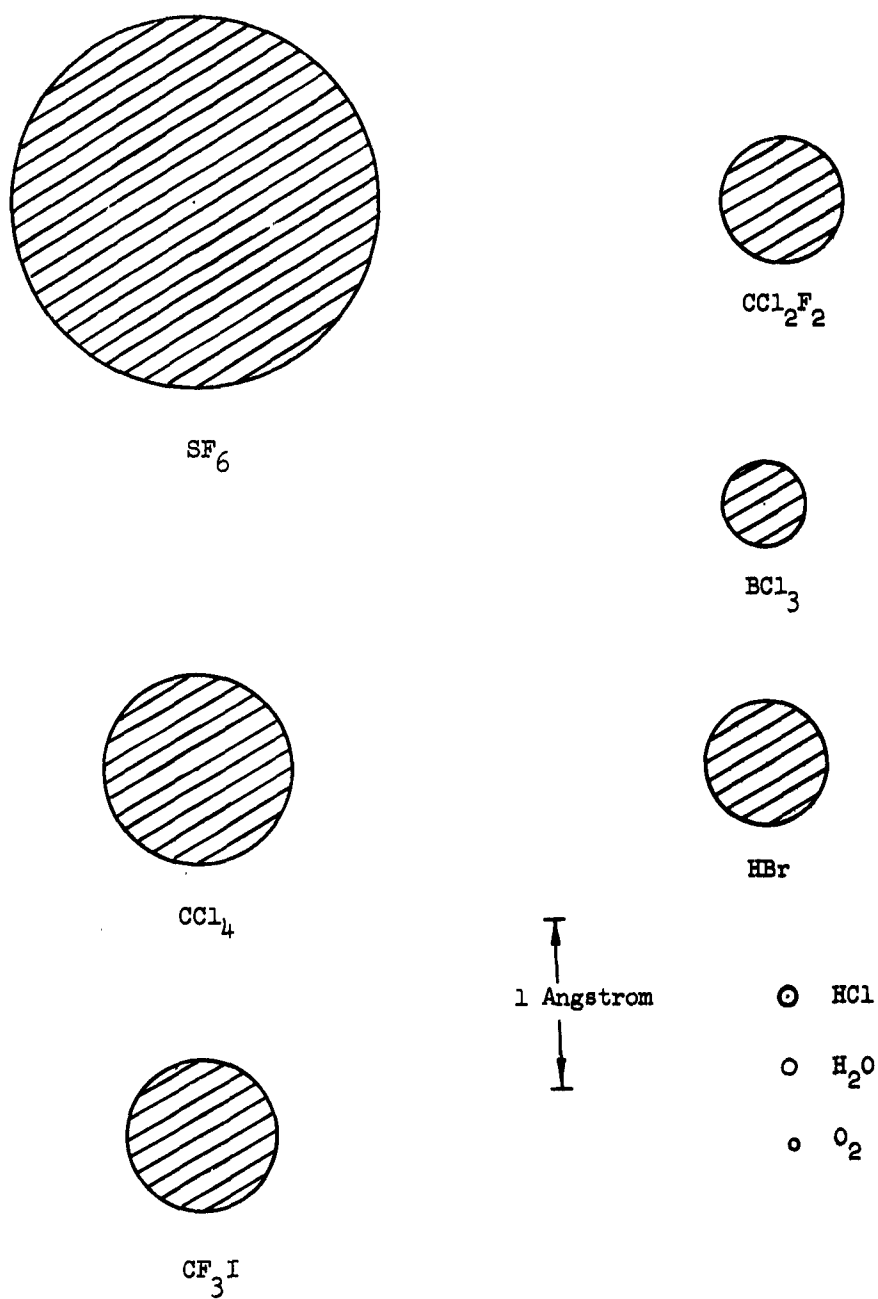
SF$_6$

CCl$_2$F$_2$

BCl$_3$

CCl$_4$

HBr

1 Angstrom

⊙   HCl
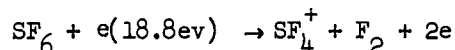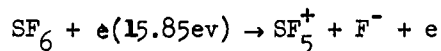
o   H$_2$O

o   O$_2$

CF$_3$I

Fig. 4.   Attachment cross-sections for zero-velocity electrons
for electronegative gases.

This means that electronegative gases are effective buildup-inhibitors primarily for very slow electrons. Once the electron has acquired more than a few eV energy, it will not become attached unless it is slowed down again.

Ionizing Collisions and Collision Products

Of the many reactions be..ween free electrons and SF_6 molecules, few can lead to carrier multiplication as required for discharge buildup. These reactions are:

$$SF_6 + e(0\text{-}2ev) \rightarrow SF_6^- \quad (\text{attachment})$$

$$SF_6 + e(2ev) \rightarrow SF_5^- + F$$

$$SF_6 + e(15.85ev) \rightarrow SF_5^+ + F^- + e$$

$$SF_6 + e(18.8ev) \rightarrow SF_4^+ + F_2 + 2e$$
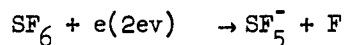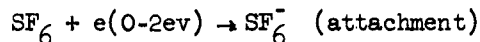
Of these reactions, only the last produces electron multiplication and, thus, is the only one which can contribute to discharge growth. There are other less important reactions in addition to those listed but, again, these do not produce electron multiplication.

Since relatively high electron energy is required to produce ionization which leads to charge multiplication, it appears that the ionization coefficient for SF_6 is low even under high fields. With a high attachment coefficient, then the value of ν_{net} should be unusually low, perhaps lower than is indicated by observed breakdown levels. This indicates a need for more theoretical investigation of SF_6 breakdown. It also leads to the speculation that impurity gases

in SF_6 may have a significant role in the breakdown mechanism. This is discussed in the next section.

Possible Effects of Impurity Content

The impurities contained in commercial sulfur hexafluoride constitute a substantial partial pressure of non-attaching gases. Both U. S. manufacturers specify a purity of 98-99[*] with the remaining 1-2% consisting of

    moisture - 0.014 - 0.002%
    air   - 0.75 - 1.1%
    SF_4 - ~ 0.2%
    so-called "high boilers" - 0 -0.0005%

Known decomposition products in the presence of air and moisture are:

    SOF_2 SO_2F_2; OF_2

    HF; S_2F_{10}; SF_4

Assuming 1% contaminant concentration of non-attaching character, this corresponds in 2 atm of SF_6 to a partial pressure of 15mm Hg. It is curious to note that this is near the Paschen minimum. It may be that the contaminants are the principal participants in the discharge process. Studies of the effects of impurity gases have been made[12,13], but these have not been extended to regions of high purity.

*Matheson Co. and Gen. Chem. Corp.
In one case, an unsubstantiated claim of 99.9% purity is made.

REFERENCES

1.   M. A. Herlin and S. C. Brown, Phys. Rev. 74, 291 (1948)

2.   A. D. McDonald and S. C. Brown, Phys. Rev. 75, 411 (1949)

3.   J. A. Pinn, Proc. Inst. of Elect. Engrs. (London) 96, 117 (1949)

4.   L. Gould and L. W. Roberts, J. Appl. Phys. 27, 1162 (1956)

5.   D. J. Rose and S. C. Brown, J. Appl. Phys. 28, 561 (1957)

6.   A. D. Mac Donald, Proc. I.R.E. 47, 436 (1959)

7.   D. J. Rose and S. C. Brown, J. Appl. Phys. 23, 711 (1952)

8.   D. J. Rose and S. C. Brown, J. Appl. Phys. 23, 718 (1952)

9.   von Engle, A.   Handbuch der Physik, Springer Verlog,
                504, Vol. 21, Berlin (1956)

10.   Pauling, L., Nature of the Chemical Bond, Cornell University
                Press, 1949

11.   Fox, R. E., J. Chem. Phys. 35, 1379 (1961)

12.   Gross, M. J., Amer. J. Ront. and Rad. Therapy, 65, 103 (1951)

13.   Howard, P. R., Proc. I.E.E. (London) 104, 123 (1957)

DISTRIBUTION LIST FOR CONTRACT REPORTS

	Copy No.
RADC (RALTP), ATTN: W. Quinn Griffiss AFB NY	1-3
RADC (RAAPT) Griffiss AFB NY	4
RADC (RAALD) Griffiss AFB NY	5
GEEIA (ROZMCAT) Griffiss AFB NY	6
RADC (RAIS, ATTN: Mr. Malloy) Griffiss AFB NY	7
U. S. Army Electronics R&D Labs RADC Griffiss AFB NY	8
AUL (3T) Maxwell AFB Ala	9
ASD (ASAPRD) Wright-Patterson AFB Ohio	10
Chief, Naval Research Lab ATTN: Code 2027 Wash 25 DC	11
Air Force Field Representative Naval Research Lab ATTN: Code 1010 Wash 25 DC	12
Commanding Officer U. S. Army Electronics R&D Labs ATTN: SELRA/SL-ADT Ft. Monmouth NJ	13
National Aeronautics & Space Admin Langley Research Center Langley Station Hampton Virginia ATTN: Librarian	14

Redstone Scientific Information Center
US Army Missile Command
Redstone Arsenal, Alabama   15

Commandant
Armed Forces Staff College (Library)
Norfolk 11 VA   16

ADC (ADOAC-DL)
Ent AFB Colo   17

AFFTC (FTOOT)
Edwards AFB Calif   18

Commander US Naval Ordnance Lab (Tech Lib)
White Oak, Silver Springs Md   19

Commanding General
White Sands Missile Range
New Mexico
ATTN: Technical Library   20

Director
US Army Engineer R&D Labs
Technical Documents Center
Ft Belvoir Va   21

ESD (ESRL)
L G Hanscom Fld
Bedford Mass   22

Commanding Officer & Director
US Navy Electronics Lab (LIB)
San Diego 52 Calif   23

ESD (ESAT)
L G Hanscom Fld
Bedford Mass   24

Commandant
US Army War College (Library)
Carlisle Barracks Pa   25

APGC (PGAPI)
Eglin AFB Fla   26

AFSWC (SWOI)
Kirtland AFB NMex   27

AFMTC (Tech Library MU-135)
    (MTBAT)
Patrick AFB Fla   28

Central Intelligence Agency
ATTN: OCR Mail Rood
2430 E Street NW
Wash 25 DC   29

US Strike Command
ATTN: STRJ5-OR
Mac Dill AFB Fla   30

AFSC (SCSE)
Andrews AFB
Wash 25 DC   31

Commanding General
US Army Electronic Proving Ground
ATTN: Technical Documents Library
Ft Huachuca Ariz   32

ASTIA (TISIA-2)
Arlington Hall Station
Arlington 12 Va   33

AFSC (SCFRE)
Andrews AFB
Wash 25 DC   34

Hq USAF (AFCOA)
Wash 25 DC   35

AFOSR (SRAS/Dr. G. R. Eber)
Holloman AFB NMex   36

Office of Chief of Naval Operations (Op-724)
Navy Dept
Wash 25 DC   37

Commander
US Naval Air Dev Cen (NADC Lib)
Johnsville Pa   38

Commander
Naval Missile Center
Tech Library (Code No. 3022)
Pt. Mugu Calif   39

Bureau of Naval Weapons
Main Navy Bldg
Wash 25 DC
ATTN: Technical Libraria, DL1-3   40

RTD (RTH)
Bolling AFB
Wash 25 DC   41

Space Sciences, Inc.
ATTN: Dr. Joseph Proud
2 Mercer Road
Natick, Massachusetts   42

Microwave Associates, Inc.
ATTN: Dr. Meyer Gilden
Burlington, Massachusetts   43